

## Perspective

Klaus Jäger\*, Johannes Sutter, Martin Hammerschmidt, Philipp-Immanuel Schneider and Christiane Becker\*

# Prospects of light management in perovskite/silicon tandem solar cells

<https://doi.org/10.1515/nanoph-2020-0674>

Received December 28, 2020; accepted February 16, 2021;  
published online March 12, 2021

**Abstract:** Perovskite/silicon tandem solar cells are regarded as a promising candidate to surpass current efficiency limits in terrestrial photovoltaics. Tandem solar cell efficiencies meanwhile reach more than 29%. However, present high-end perovskite/silicon tandem solar cells still suffer from optical losses. We review recent numerical and experimental perovskite/silicon tandem solar cell studies and analyse the applied measures for light management. Literature indicates that highest experimental efficiencies are obtained using fully planar perovskite top cells, being in contradiction to the outcome of optical simulations calling for textured interfaces. The reason is that the preferred perovskite top cell solution-processing is often incompatible with usual micropylamidal textures of silicon bottom cells. Based on the literature survey, we propose a certain gentle nanotexture as an example to reduce optical losses in perovskite/silicon tandem solar cells. Optical simulations using the finite-element method reveal that an

intermediate texture between top and bottom cell does not yield an optical benefit when compared with optimized planar designs. A double-side textured top-cell design is found to be necessary to reduce reflectance losses by the current density equivalent of 1 mA/cm<sup>2</sup>. The presented results illustrate a way to push perovskite/silicon tandem solar cell efficiencies beyond 30% by improved light management.

**Keywords:** light management; perovskite/silicon tandem solar cells; perovskite solar cells.

## 1 Introduction

Silicon solar cells currently dominate the photovoltaics (PV) sector with more than 90% market share [1]. They achieved power conversion efficiencies (PCEs) of 26.7% [2] approaching the theoretical limit for silicon solar cells of 29.4% [3]. Perovskite/silicon tandem solar cells are regarded as one of the most promising concepts to surpass this limit at low costs. Adding a perovskite solar cell on top of a silicon solar cell allows to harvest the high-energy part of sunlight with lower losses pushing the physical limit efficiency towards around 44% [4]. Recently, perovskite/silicon tandem solar cells with PCEs exceeding 29% were presented [5, 6], significantly outperforming the record silicon record cell.

Light management has been identified as crucial in perovskite/silicon tandem solar cell devices [7, 8]. Optical engineering in solar cells always comprises – independent of the absorber material and configuration – (1) measures for broadband reflection reduction and (2) concepts to minimize parasitic absorption in functional (contact) layers. Further, in case of poorly absorbing solar cell materials, such as crystalline silicon or very thin absorber layers, light cannot be absorbed completely at a single or double pass through the layer. In this case also (3) measures to increase the light path in the absorber layer have to be taken, known by the term “light trapping”. As

---

\*Corresponding authors: Klaus Jäger, Helmholtz-Zentrum Berlin für Materialien und Energie GmbH, Department Optics for Solar Energy, Berlin, Germany; and Zuse Institute Berlin, Computational Nano Optics, Berlin, Germany, E-mail: klaus.jaeger@helmholtz-berlin.de. <https://orcid.org/0000-0002-6008-9559>; and Christiane Becker, Helmholtz-Zentrum Berlin für Materialien und Energie GmbH, Department Optics for Solar Energy, Berlin, Germany, E-mail: christiane.becker@helmholtz-berlin.de. <https://orcid.org/0000-0003-4658-4358> (C. Becker)

Johannes Sutter, Helmholtz-Zentrum Berlin für Materialien und Energie GmbH, Department Optics for Solar Energy, Berlin, Germany, E-mail: johannes.sutter@helmholtz-berlin.de. <https://orcid.org/0000-0001-5634-3449>

Martin Hammerschmidt and Philipp-Immanuel Schneider, JCMwave GmbH, Berlin, Germany; and Zuse Institute Berlin, Computational Nano Optics, Berlin, Germany. E-mail: martin.hammerschmidt@jcmwave.com (M. Hammerschmidt). <https://orcid.org/0000-0003-0291-1599> (M. Hammerschmidt), E-mail: philipp.schneider@jcmwave.com (P.-I. Schneider). <https://orcid.org/0000-0002-9949-9483> (P.-I. Schneider)

perovskites have high absorption coefficients, light trapping plays a minor role in perovskite single-junction solar cells. In perovskite/silicon tandem solar cells, however, light trapping is important for the silicon bottom cell. In case of monolithic tandem solar cells where the perovskite and silicon subcells are connected in series, a fourth optical engineering task comes into play: (4) splitting the solar spectrum in such a way that both subcells absorb the same amount of photons to ensure current matching.

In established solar cell technologies based on non-perovskite absorbers, these optical engineering measures are mostly taken by a combination of anti-reflective layers and texturing of interfaces. Textures are optically beneficial in two ways: first, they exhibit a broadband anti-reflective effect by giving the light the opportunity to enter the absorber layer multiple times in case of microtextures [9] or by reduced reflectance owing to a graded index effect in case of sub-wavelength scale structures [10]. Second, textures with typical feature sizes ranging from hundreds of nanometers to several micrometers scatter the light and hence increase average light path and absorption in the absorber layers. For instance, in amorphous and microcrystalline silicon thin-film solar cells textured transparent conductive layers were used for light trapping [11], while high-efficient monocrystalline silicon solar cells mostly exhibit a double-side textured wafer with micrometer-sized pyramids [12] covered with an anti-reflective layer.

In this article, we first summarize and classify relevant literature on light management in monolithic perovskite/silicon tandem solar cells. We discuss why experimental high-end tandem solar cells often do not use the optical concepts which would be ideal according to numerical studies based on optical simulations. We put an emphasis on the analysis of textured interfaces for broadband light management and discuss their constraints for experimental production. With the configuration of the current perovskite/silicon record tandem solar cell as a starting point, we numerically propose gentle nanotextures for light management meeting all optical and experimental requirements to push PCEs of perovskite/silicon tandem solar cells beyond 30%.

## 2 Literature overview

Most highly efficient silicon solar cells have a pyramidal microtexture on the front side. From an industrial perspective such a device would be an ideal starting point for adding a perovskite cell on top to form a tandem device. Also from an optical point of view this makes

sense: many numerical studies predict excellent optical absorption, when the perovskite top cell is conformally deposited on top of such a microtextured silicon bottom cell: Schneider et al. [13] and Shi et al. [14] simulated the optical properties of perovskite/silicon tandem solar cells with inverted pyramidal texture in combination with an adapted intermediate layer between top and bottom cell supporting the great optical potential of such a fully textured perovskite absorber. Also Santbergen et al. [15], Lehr et al. [16], Jacobs et al. [7], Qaroni et al. [17] and Subhan et al. [18] reported that a fully textured perovskite top cell, conformally grown on pyramidally microtextured silicon, yields the highest absorption, particularly when compared to configurations with partly planar perovskite interfaces. Chen et al. came to a similar conclusion using a sub-micrometer sinusoidal texture at the silicon bottom cell front side [19]. From an optical simulation point of view the situation is clear: a double-side textured perovskite top cell on top of a double-side textured silicon bottom-cell yields the best optical performance.

Table 1 summarizes *experimentally* realized monolithic perovskite/silicon tandem solar cells with a PCE exceeding 25% and their relevant optical parameters. In contrast to the results of the optical simulations discussed above, the best device with available details on the solar cell configuration with 29.15% PCE [5] relies on a fully planar perovskite top cell. The reason is that – as of early 2021 – spin-coating yields the perovskite materials with the highest optoelectronic quality. This also includes the currently best perovskite single-junction device with 25.2% PCE [2]. In a monolithic tandem device, the perovskite top cell has to be manufactured on top of the silicon bottom cell. Unfortunately, solution-processing of sub-micrometer thin perovskite layers is incompatible with state-of-the-art pyramidal microtextures on the silicon bottom cell. Although planar interfaces are not ideal from an optical point of view, new developments yielded a remarkable efficiency improvement. They can be classified in two categories and are sketched in Figure 1(a). First, a planar optical interlayer consisting of nanocrystalline silicon oxide (nc-SiO<sub>x</sub>) with adjusted refractive index was applied between silicon and perovskite. This configuration yielded a short circuit current density ( $J_{sc}$ ) gain by 1.4 mA/cm<sup>2</sup> in the silicon bottom cell [22] [Configuration **A** in Table 1 and Figure 1(a)] – with  $J_{sc}$  being the solar cell parameter directly reflecting optical absorption and hence the amount of generated free carriers. In the second approach illustrated in Figure 1(a), a textured light scattering foil is put on top of the front side of the

**Table 1:** Summary of recent high-efficient monolithic perovskite/silicon tandem solar cells with PCE  $\eta > 25\%$  and their light management strategies (see also Figure 1): **A** denotes a nc-SiO<sub>x</sub> interlayer, **B** a textured front foil at the air-glass interface, **C** a double-side textured perovskite absorber layer, and **D** a single-sided textured perovskite absorber.  $J_{sc,JV}$  denotes the short circuit current density ( $J_{sc}$ ) as determined from  $JV$ -characteristics,  $J_{sc,EQE\ top/bot/R}$  constitutes the  $J_{sc}$  values as calculated from external quantum efficiency (EQE) data of perovskite top and silicon bottom cell, as well as reflectance losses, respectively. All  $J_{sc}$  values are given in mA/cm<sup>2</sup>.

Reference <sup>a</sup>		$\eta$ [%]	$J_{sc,JV}$	$J_{sc,EQE\ top}$	$J_{sc,EQE\ bot}$	$\sum J_{sc,EQE}$	$J_{sc,R}$	Configuration
(I) Fully planar perovskite absorber layer								
Bush et al. (2018)	[20]	25.0	18.4	18.4	18.5	36.9	4.2 <sup>b</sup>	–
Jost et al. (2018)	[21]	25.5	18.5	20.2	18.8	39.0	2.5	B
Mazzarella et al. (2019)	[22]	25.2	19.0	19.9	18.8	38.7	≈2.5	A
Köhnen et al. (2019)	[23]	26.0	19.2	20.2	19.3	39.5	3.5	A
Al-Ashouri et al. (2020)	[5]	29.1	19.8	19.4	20.2	39.6	2.6	A
Xu et al. (2020)	[24]	27.1	19.1	19.3	19.9	39.2	–	B
(II) Textured perovskite absorber layer								
Sahli et al. (2018)	[25]	25.2	19.5	20.1	20.3	40.4	1.2 <sup>b</sup>	C
Nogay et al. (2019)	[26]	25.1	19.5	19.7	20.0	39.7	–	C
Hou et al. (2020)	[27]	25.7	19.3	19.3	19.2	38.7	2.5 <sup>b</sup>	D
Chen et al. (2020)	[28]	26.0	19.2	19.3	19.4	38.7	2.3	B + D
Aydin et al. (2020)	[29]	25.1	19.8	19.8	19.8	39.6	1.4 <sup>b</sup>	C

<sup>a</sup> 29.5% world record device by OxfordPV [6] from 21 Dec 2020 not considered due to missing available data.

<sup>b</sup> 1 – R data digitized from the respective publication.

device, leaving the perovskite solar cell unaffected, *i.e.*, planar. Such textured foils strongly increase photocurrent densities in two-terminal perovskite/silicon tandem solar cells, particularly under diffuse illumination conditions [21, 24, 28] [Configuration **B** in Table 1 and Figure 1(a)]. Jaysankar et al. used similar attachable textured foils in four-terminal perovskite/silicon tandem solar cells and attributed the optical benefit to reduced reflection losses [30]. The sum of the short circuit current densities as extracted from EQE measurements of top and bottom cells amounts to values between 36.9 mA/cm<sup>2</sup> and 39.6 mA/cm<sup>2</sup> in case of the device by Al-Ashouri et al. [5], which suffers reflectance-induced current losses of 2.6 mA/cm<sup>2</sup> only. For comparison, all sunlight in the range between 300 and 1200 nm would yield 46.5 mA/cm<sup>2</sup>. The obtained current densities are remarkable because they are obtained with fully planar perovskite top cells.

A very interesting evolution are textured perovskite absorber layers. They can be realized either by developing alternative perovskite deposition methods that are compatible with micrometer-sized standard light management textures [25, 26, 29], or by adapting the texture feature size on the front side of the silicon solar cell and the perovskite absorber thickness such that solution-processed textured perovskite layers become feasible [27, 28, 31], as illustrated in Figure 1(b). The works by Sahli et al. [25] and subsequent studies [26, 29] stand out from all

the other studies for several reasons: These are the only works on a monolithic perovskite/silicon tandem solar cell with a fully textured perovskite top cell. This is the preferred configuration from an optical point of view and also has the best compatibility with industry-scale silicon bottom cells with pyramidal front texture [Configuration **C** in Table 1 and Figure 1(b)]. Also the sum of the current densities as extracted from EQE measurements reach up to 40.4 mA/cm<sup>2</sup>, which results from strongly reduced reflection losses amounting to around 1.2–1.4 mA/cm<sup>2</sup> only. The conformal growth of the perovskite layer became possible by a hybrid two-step deposition method, which combines sequential co-evaporation and spin-coating. Due to small deficiencies in open circuit voltage and fill factor, the efficiency remained at 25.2%. In contrast, Hou et al. [27], Chen et al. [28] and Subbiah et al. [31] managed to achieve single-side textured perovskite top cells on top of a double-side textured silicon bottom cell by applying the preferred solution-processing of perovskite layers on small-scale pyramids by spin-coating, blade-coating and slot-die-coating, respectively [Configuration **D** in Table 1 and Figure 1(b)]. Chen et al. additionally applied a scattering foil (Configuration **B**). The solar cells reported by Hou and Chen exhibit comparably thick perovskite layers and cumulative current densities of 38.7 mA/cm<sup>2</sup> and efficiencies in the range of 26%. Figure 1 depicts one representative

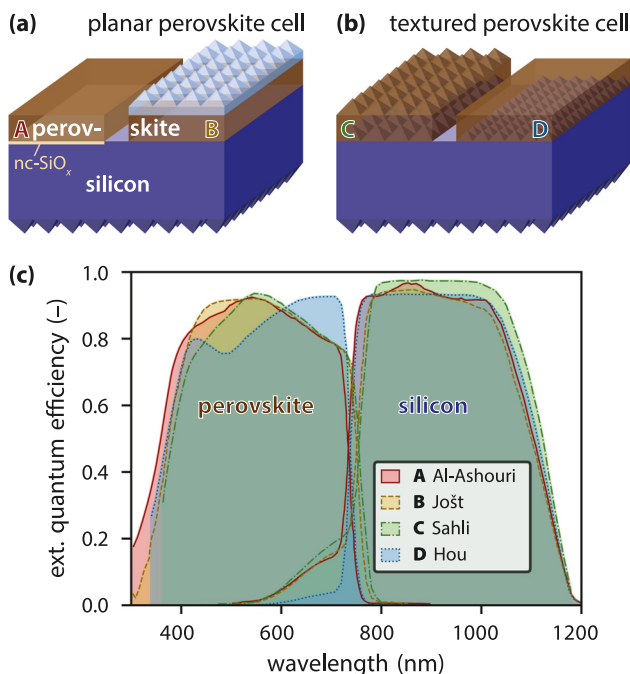


**Figure 1:** Experimental results for perovskite/silicon tandem solar cells with different optical concepts. (a) Solar cells with a planar perovskite top cell with **A**, a nanocrystalline silicon oxide ( $\text{nc-SiO}_x$ ) interlayer and with **B**, a textured foil on top. (b) Tandem solar cell with textured perovskite layers, where the perovskite layer is either **C** fully textured or **D** just textured on the rear side. (c) Best experimental results representing the four architectures illustrated in (a) and (b): **A** intermediate  $\text{nc-SiO}_x$  layer (Al-Ashouri et al. [5]), **B** planar perovskite cell with textured foil on top (Jošt et al. [21]), **C** fully textured perovskite cell (Sahli et al. [25]), and **D** perovskite cell with textured back and planar front (Hou et al. [27]).

of each of the four light management strategies **A–D**. Texturing (**C** & **D**) helps to maximize the EQE of the silicon bottom-cell, which becomes particularly visible at wavelengths longer than 800 nm. Also for the perovskite top cell, the double-side textured device (**C**) shows the highest absolute EQE values. A textured foil attached at the front side of the tandem device (**B**) bears the potential to further increase EQE of both sub-cells.

In summary, in order to push efficiencies of perovskite/silicon tandem solar cells beyond 30%, we regard implementing a double-side textured perovskite top cell mandatory for good light management.

Now as we established that the perovskite top cell should be textured, it is worth to review the literature on textured perovskite single-junction devices. Many perovskite deposition methods were investigated, which either enable growth on micro pyramids, or alternative textures that are compatible with perovskite solution

processing. Both approaches bear the potential for perovskite/silicon tandem solar cells exceeding 30% PCE by improved light management. Table 2 summarizes recent studies on perovskite single-junction solar cells with a textured perovskite absorber layer. Paetzold et al. realized a first proof-of-concept device by patterning the glass substrate of the solar cell by nanoimprint lithography followed by standard spin-coating of the perovskite solar cell [33]. Shi et al. used glasses covered by textured fluorine-doped tin oxide (FTO) to enhance light absorption in thin perovskite solar cells [34]. Deng et al. used a titanium oxide layer on top of the FTO layer with a grating texture [35]. Wu et al. included plasmonic gold nanostars into the  $\text{TiO}_x$  layer [36] and Tockhorn et al. used glass substrates with various textures for their spin-coated perovskite solar cells [37]. Up to 21.6% single-junction PCEs were realized by Xu et al. using a textured polymer layer in combination with an anti-reflective coating on glass [38]. In all these devices, the perovskite absorber layer exhibits a textured front side, but a flat rear side.

In contrast, Schmager et al. applied high-pressure thermal nanoimprint lithography to realize perovskite solar cells with a textured rear side [39]. As discussed above, the optimal case would be a perovskite solar cell which was conformally deposited onto a silicon bottom cell with a pyramidally microtextured surface. A pyramidal double-side textured perovskite cell would supersede other configurations in both, the optical absorption and with regard to the compatibility with state-of-the-art silicon solar cells. A first study on fully vacuum processed perovskite solar cells on pyramidal microtextured glass was recently published by Gil-Escrig et al. [40]. All these studies contain valuable insights in light management textures for perovskite solar cells. When comparing the values of the short circuit current densities as extracted from EQE measurements  $J_{\text{sc,EQE}}$  three studies stand out with large  $J_{\text{sc,EQE}}/J_{\text{max}}$  ratios in the range of 90%.  $J_{\text{max}}$  describes the maximum attainable short circuit current density according to the optically active perovskite bandgap, which was determined from the minimum in the derivative of the EQE plots [32] from the respective publication. Interestingly, the three best performing devices exhibit textures in very different sizes: micrometer-sized in the case of Deng et al. [35], comparable to the wavelength in case of Tockhorn et al. [37], and smaller than the wavelength by Xu et al. [38]. It seems that the texture size plays a minor role – if a texture is present. According to the current knowledge, we regard these three approaches yielding efficiencies in the range of 20% as promising for perovskite/silicon tandem solar cells with PCEs exceeding 30%.

**Table 2:** Summary of recent perovskite single-junction solar cells with nano- or micro-textured absorber layers for light management.  $J_{sc,JV}$  and  $J_{sc,EQE}$  denote the short circuit current density ( $J_{sc}$ ) as determined from  $JV$ -characteristics and EQE, respectively.  $J_{sc,EQE}/J_{max}$  denotes the ratio of  $J_{sc,EQE}$  to the maximum attainable short circuit current density ( $J_{max}$ ) according to the respective perovskite bandgap (the approximate optically active bandgap of the perovskite was determined from the minimum in the derivative of the EQE [32], which where digitized from the respective publication). All  $J_{sc}$  values are given in  $\text{mA}/\text{cm}^2$ .

Reference		$\eta$ [%]	$J_{sc,JV}$	$J_{sc,EQE}$	$J_{sc}/J_{max}$	Texture details
(I) Textured front side						
Paetzold et al. (2015)	[33]	9.9	–	19.4	78.4%	Textured ITO, 500 nm pitch
Shi et al. (2017)	[34]	13.3	19.8	18.7 <sup>b</sup>	75.8%	Textured FTO
Deng et al. (2019)	[35]	19.6	24.2	22.0	89.2%	1.5 $\mu\text{m}$ -periodic grating in TiOx
Wu et al. (2020)	[36]	20.0	22.3	19.4 <sup>b</sup>	81.0%	Plasmonic gold nanostars in TiOx
Tockhorn et al. (2020) <sup>a</sup>	[37]	19.7	22.8	23.1	93.5%	Sinusoidal textured glass, 750 nm pitch
Xu et al. (2020)	[38]	21.6	23.3	22.2	89.5%	Textured polymer, 40–120 nm features
(II) Textured rear side						
Schmager et al. (2019)	[39]	14.8	19.4	19.5 <sup>b</sup>	78.5%	Textured perovskite, 480 nm pitch
(III) Fully textured perovskite layer						
Gil-Escrig et al. (2020)	[40]	15.4	20.2	21.0	81.4%	Micro-pyramids

<sup>a</sup> Selected texture for numerical study of Section 3.

<sup>b</sup>  $J_{sc,EQE}$  calculated from digitized EQE plot.

### 3 Perovskite/silicon tandem solar cells with gentle nanotextures

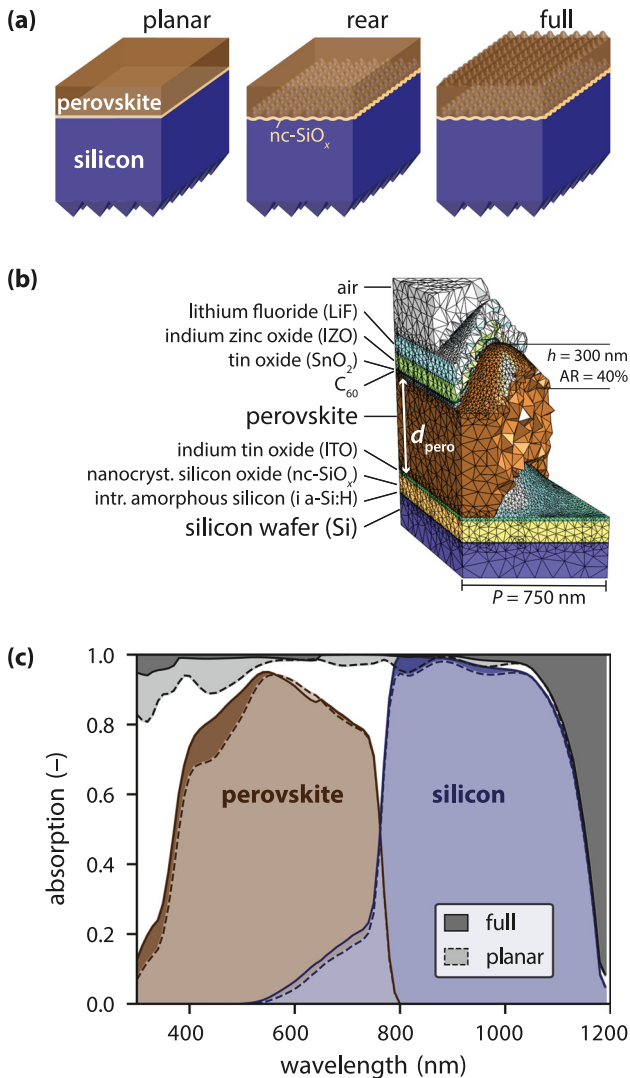
With the knowledge gained in Section 2, we now study how sinusoidal nanotextures can improve the light management in perovskite/silicon tandem solar cells. We believe that this approach is promising for the following reasons: first, the demonstrated short circuit current densities of sinusoidally textured perovskite solar cells approach one of the highest values when compared to the maximum attainable current density for the respective perovskite bandgap, proving excellent light management capabilities [37] (see Table 2). The absolute efficiencies of perovskite solar cells with such textures approach 20%, which is necessary to obtain high tandem solar cell efficiencies. Further, such textures have already been successfully transferred into the front side of silicon bottom cells without deteriorating the carrier lifetime in the silicon [41]. Last, numerical studies have demonstrated the high theoretical potential of sinusoidal nanotextures [19, 42]. Please note that also an inverse pyramid texture would fulfill the requirements of compatibility with spin-coated perovskite top cells [37] and high-quality silicon bottom cells [43]. However, in this study we focus on sinusoidal structures as an example.

Figure 2 shows details of a numerical study for three configurations of perovskite/silicon tandem devices

illustrated in Figure 2(a): with a planar perovskite top cell, with a perovskite top cell with nanotextures on its rear, and with a fully textured perovskite top cell. The simulations were performed with the finite element solver JCMsuite [49]. A typical mesh for the device with a fully textured perovskite cell is shown in Figure 2(b). As nanotextures, we used “negative cosine” sinusoidal nanotextures with periods ranging from 500 to 1000 nm and aspect ratios between 0.2 and 0.6, where the aspect ratio is the ratio between the height and the period of the nanotexture.

Details on the layer stack are given in Figure 2(b) and Table 3. It is based on the solar cell design by Al-Ashouri et al., which yielded 29.1% PCE [5]. As we do not have optical data for their new perovskite material  $\text{Cs}_{0.05}(\text{FA}_{0.77}\text{MA}_{0.23})_{0.95}\text{Pb}(\text{I}_{0.77}\text{Br}_{0.23})_3$  with 1.68 eV bandgap, we performed the simulations with optical data for the triple-cation perovskite  $\text{Cs}_{0.05}(\text{MA}_{0.17}\text{FA}_{0.83})\text{Pb}(\text{I}_{0.83}\text{Br}_{0.17})_3$  with  $\approx 1.64$  eV bandgap instead. A self-assembling monolayer between ITO and perovskite can be omitted in the optical simulations.

All simulations were performed for the wavelength range between 300 and 1190 nm. In the simulations, only a 100 nm-thin silicon layer was considered with adjoined perfectly matched silicon layer, hence infinitely thick silicon at the back. To account for the finite thickness of



**Figure 2:** Numerical results on the optical performance of perovskite/silicon tandem cells with either a planar front side, a rear-side textured perovskite cell or a fully textured perovskite cell. Illustrations of the simulated devices are shown in (a), the simulated absorption data for the perovskite and silicon layers of the optimized devices are plotted in (c). The simulations were performed with the finite element method, a typical mesh for a fully-textured device with 750 nm period and 300 nm texture height (equivalent to 40% aspect ratio) is shown in (b). For all devices Lambertian light trapping is considered at the back of the silicon cell. For clarity, the curves for the rear-side textured device are omitted in (c), because they can hardly be distinguished from the curves for the planar device. These results are given in Figure S3 of the Supplementary Materials.

the silicon wafer ( $d_{\text{Si}} = 300 \mu\text{m}$ ), we corrected the absorption in silicon using the Tiedje–Yablonoitch limit [50], which assumes perfect (Lambertian) light trapping in silicon, which for example can be reached by a textured silicon back side:

$$A_{\text{Si, corr}}(\lambda) = A_{\text{Si}}(\lambda) \frac{\alpha(\lambda)}{\alpha(\lambda) + [4d_{\text{Si}}n^2(\lambda)]^{-1}}. \quad (1)$$

In Eq. (1),  $A_{\text{Si}}$  is the absorption in Si as obtained from the FEM simulation,  $\alpha$  denotes the absorption coefficient of silicon,  $n$  is the real part of the refractive index and  $d_{\text{Si}}$  is the wafer thickness.

In order to explore the full potential of the studied device designs, we optimized several layer thicknesses of perovskite/silicon tandem solar cells. We employed Bayesian optimization included in JCMsuite’s optimization toolbox. This global optimization method starts at a random initial point. At each iteration, it employs a stochastic model (a Gaussian process) trained with all previous function evaluations to determine new parameter values with a large expected improvement. The method has proven to be highly efficient for the shape optimization of photonic structures [51]. The optimization objective was to maximize the minimum of the photon-current densities generated by the two subcells,  $\max[\min(J_{\text{ph, pero}}(\text{par.}), J_{\text{ph, Si}}(\text{par.}))]$ . The photon-current densities were calculated as in Ref. [19]. This objective function has the advantage that it minimizes the reflection and parasitic absorption losses while it reaches current matching at the same time [47].

For the optimization of the planar solar cell, we allowed three layer thicknesses to vary: the nc-SiO<sub>x</sub> intermediate layer, the perovskite absorber, and the lithium fluoride (LiF) front antireflective layer – more information on this optimization is given in Figure S1 in the Supplementary Materials document. In earlier optimizations, we also allowed the indium zinc oxide (IZO) layer to vary. However, as the IZO layer thickness always moves to the set minimal value during optimization, we kept it fixed at 90 nm, because for thinner IZO layers the sheet resistance increases and series-resistance losses would become too large.

As simulation of textured solar cells is much more time consuming, we restricted the number of free parameters. For optimizing the device with the rear-side textured perovskite cell, we set the LiF thicknesses to the value found by optimizing the planar layer stack and allowed the nc-SiO<sub>x</sub> and perovskite layer thicknesses to vary, because we can assume that texturing the interfaces between perovskite and silicon does not affect the optimal layer thicknesses between perovskite and air. We performed this optimization for 750 nm period and 40% aspect ratio. From this optimization, which is summarized in Figure S2 of the Supplementary Materials document, we learned that the nc-SiO<sub>x</sub> thickness hardly affects the optical performance. For the device with a fully textured top cell and for all the other periods and aspect ratios,

**Table 3:** The materials and layer thicknesses used for the optical simulations shown in Figure 2. All thicknesses (except Si) are given in nm, the italic thicknesses resulted from an optimization, and the underlined values were taken from a previous optimization. The sources for refractive index data are given. Further, the photo-current densities in the perovskite and silicon cells as well as the reflective losses are shown – for the textured devices the data are for nanotextures with 750 nm period and 40% aspect ratio. For other periods and aspect ratios, all layer thicknesses are the same except for perovskite.

		Planar	Rear	Full
Lithium fluoride (LiF)	[44]	110	<u>110</u>	<u>110</u>
Indium zinc oxide (IZO)	[21]	90	90	90
Tin oxide (SnO <sub>2</sub> )	[21]	10	10	10
C <sub>60</sub>	[45]	23	23	23
Cs <sub>0.05</sub> (MA <sub>0.17</sub> FA <sub>0.83</sub> )Pb(I <sub>0.83</sub> Br <sub>0.17</sub> ) <sub>3</sub> (perovskite)	[45]	569	594 <sup>a</sup>	563
Indium tin oxide (ITO)	[45]	21	21	21
Nanocrystalline silicon oxide (nc-SiO <sub>x</sub> )	[46]	107	109	<u>109</u>
Intrinsic amorphous hydrogenated Si (a-Si:H)	[47]	5	5	5
Crystalline silicon (wafer, Si)	[48]	300 μm	300 μm	300 μm
$J_{ph, pero}$ (mA/cm <sup>2</sup> )		20.3	20.3	21.0
$J_{ph, Si}$ (mA/cm <sup>2</sup> )		20.3	20.3	21.0
$J_{ph, refl}$ (mA/cm <sup>2</sup> )		3.1	3.0	2.0

<sup>a</sup>For the rear-textured device, the perovskite layer is not conformal. Here, the thickness denotes the thickness of a planar layer with the same volume.

we therefore only varied the perovskite thickness to reach current matching using Newton's method, as described previously [19]. During all these simulations, we observed that changing the perovskite thickness does not affect the photon-current density  $J_{ph, refl}$  lost by reflection.

Figure 2(c), Figure S3 in the Supplementary Material and Tables 3 and 4 show the results for the optimized device stacks. Most strikingly, the planar and rear-textured devices have almost similar current densities and reflection losses. For wavelength shorter than 500 nm, the absorption curves cannot be distinguished because no light reaches the back of the perovskite layer and the layer stack on front is equal. For larger wavelength, the absorption curves are very close to each other. This is in contrast to the results discussed in reference [19], where a rear-side textured device with 40% aspect ratio gained around 0.5 mA/cm<sup>2</sup> photocurrent density with respect to the planar reference. In contrast to this older study, the devices studied in this work have a nc-SiO<sub>x</sub> intermediate layer with excellent optical properties [46]. Hence, nano-texturing the interfaces between the silicon wafer and the perovskite layer does not improve the device from an optical point of view, if a nc-SiO<sub>x</sub> layer is present. With these kind of simulations, we cannot take the back side of the silicon wafer into account. Hence, it is not possible to determine whether texturing the rear side of the perovskite induces additional light trapping in the silicon sub cell.

The device with a fully textured perovskite cell supersedes the devices with a flat front, as it has a

antireflective effect over the whole wavelength range reducing the reflective losses by around 0.5 and 1 mA/cm<sup>2</sup> for 20 and 40% aspect ratio, respectively. Increasing the aspect ratio to 60% only reduces the reflection by an additional 0.1 mA/cm<sup>2</sup>. Interestingly, changing the period hardly affects the reflective losses when the aspect ratio is kept constant. This agrees with the conclusion of Section 2: the texture size plays a minor role – if a texture is present. Texturing the front side would be beneficial from an optical point of view, but it is most difficult to realize for perovskite cells, as discussed in Section 2 as well.

**Table 4:** Effect of aspect ratio AR and period  $P$  of sinusoidal nanotextures on the photon-current density  $J_{ph, refl}$  lost by reflection. Results are shown for devices with a rear-side textured or fully textured perovskite top cell, as illustrated in Figure 2(a). For these simulations, the layer thicknesses were as in Table 3, except the perovskite thickness, which was adjusted to reach current matching using Newton's method.

$J_{ph, refl}$ (mA/cm <sup>2</sup> ) as function of $P$ and AR							
Texture	Aspect ratio	Rear			Full		
		20%	40%	60%	20%	40%	60%
Period	500 nm	3.1	3.0	3.0	2.5	2.0	1.9
	750 nm	3.0	3.0	3.0	2.6	2.0	1.9
	1000 nm	3.1	3.1	3.0	2.8	2.1	1.9

## 4 Conclusion

We studied the state of light management in the vibrant field of monolithic perovskite/silicon tandem solar cells. We carefully analysed the optics of recent experimentally realized high-end perovskite/silicon tandem solar cells and compared the outcome with the literature on optical simulations of suchlike devices. According to this survey, experimental high-end tandem solar cells often do not use optical concepts with textured interfaces, which would be ideal according to numerical studies based on optical simulations. This can be explained by the fact that the preferred solution-processing of perovskite top cells is incompatible with state-of-the-art silicon micro pyramid textures. By further reviewing the status of textured perovskite single junction solar cells, we identified certain textures that are compatible with perovskite solution-processing. We selected a sinusoidal nanotexture that has proven to preserve the electronic quality in both, perovskite [37] and silicon solar cells [41], and performed optical simulations based on the finite-element method to compute the performance of respectively textured perovskite/silicon tandem solar cells. We found that a single textured interface between perovskite and silicon sub cells does not yield an optical benefit when compared to optimized planar designs with an intermediate layer between the sub cells. However, conformal and hence double-side textured perovskite top cells on such a gentle sinusoidal texture reduce reflectance losses equivalent to up to 1 mA/cm<sup>2</sup> of short circuit current density. We therefore regard double-side texturing of the perovskite top-cell as a mandatory next step for future perovskite/silicon tandem solar cells and deliver concrete design criteria to push tandem solar cell efficiencies beyond 30% by advanced light management.

**Acknowledgement:** The authors thank Alvaro Tejada Esteves from Helmholtz-Zentrum Berlin für Materialien und Energie for providing them with refractive index data for ITO, perovskite and C<sub>60</sub>.

**Author contribution:** CB analysed the literature on textured perovskite (tandem) solar cells, KJ conducted the optical simulations and optimizations. JS extracted data from the studied literature. MH and PS supported the optical simulations and optimizations. CB and KJ wrote the manuscript. All authors proofread the manuscript.

**Research funding:** The authors thank the Helmholtz Association (FundRef DOI: 10.13039/501100001656) for funding within the Helmholtz Excellence Network SOLARMATH, a strategic collaboration of the DFG Excellence Cluster

MATH+ and Helmholtz-Zentrum Berlin (grant no. ExNet-0042-Phase-2-3). JS, MH and PS thank the German Federal Ministry of Education and Research (FundRef DOI: 10.13039/501100002347) for funding within the project SNaPSHoTs (grant no. 01IO1806 and 01IO1807).

**Conflict of interest statement:** The authors declare no conflicts of interest regarding this article.

## References

- [1] ITRPV, “11th edition of the International Technology Roadmap Photovoltaics,” Technical report, VDMA, 2020 [accessed: Aug. 31, 2020].
- [2] M. Green, E. Dunlop, J. Hohl-Ebinger, M. Yoshita, N. Kopidakis, and X. Hao, “Solar cell efficiency tables (version 57),” *Prog. Photovoltaics Res. Appl.*, vol. 29, no. 1, pp. 3–15, 2020.
- [3] A. Richter, M. Hermlle, and S. W. Glunz, “Reassessment of the limiting efficiency for crystalline silicon solar cells,” *IEEE J. Photovolt.*, vol. 3, no. 4, pp. 1184–1191, 2013.
- [4] T. Leijtens, K. A. Bush, R. Prasanna, and M. D. McGehee, “Opportunities and challenges for tandem solar cells using metal halide perovskite semiconductors,” *Nat. Energy*, vol. 3, no. 10, pp. 828–838, 2018.
- [5] A. Al-Ashouri, E. Köhnen, B. Li, et al., “Monolithic perovskite/silicon tandem solar cell with >29% efficiency by enhanced hole extraction,” *Science*, vol. 370, no. 6522, pp. 1300–1309, 2020.
- [6] OxfordPV, Technical report, 2020, <https://www.oxfordpv.com/news/oxford-pv-hits-new-world-record-solar-cell> [accessed: Dec. 28, 2020].
- [7] D. A. Jacobs, M. Langenhorst, F. Sahli, et al., “Light management: a key concept in high-efficiency perovskite/silicon tandem photovoltaics,” *J. Phys. Chem. Lett.*, vol. 10, no. 11, pp. 3159–3170, 2019.
- [8] Q. Xu, Y. Zhao, and X. Zhang, “Light management in monolithic perovskite/silicon tandem solar cells,” *Sol. RRL*, vol. 4, no. 2, p. 1900206, 2020.
- [9] B. Dale and H. G. Rudenberg, “High efficiency silicon solar cells,” in *Proc. 14th Annu. Power Sources Conf.*, 1960, p. 122.
- [10] J. Zhu, Z. Yu, G. F. Burkhard, et al., “Optical absorption enhancement in amorphous silicon nanowire and nanocone arrays,” *Nano Lett.*, vol. 9, no. 1, pp. 279–282, 2009.
- [11] J. Müller, B. Rech, J. Springer, and M. Vanecek, “TCO and light trapping in silicon thin film solar cells,” *Sol. Energy*, vol. 77, no. 6, pp. 917–930, 2004.
- [12] E. Vazsonyi, K. De Clercq, R. Einhaus, et al., “Improved anisotropic etching process for industrial texturing of silicon solar cells,” *Sol. Energy Mater. Sol. Cell.*, vol. 57, no. 2, pp. 179–188, 1999.
- [13] B. W. Schneider, N. N. Lal, S. Baker-Finch, and T. P. White, “Pyramidal surface textures for light trapping and antireflection in perovskite-on-silicon tandem solar cells,” *Optic Express*, vol. 22, no. S6, p. A1422, 2014.
- [14] D. Shi, Y. Zeng, and W. Shen, “Perovskite/c-Si tandem solar cell with inverted nanopillars: realizing high efficiency by controllable light trapping,” *Sci. Rep.*, vol. 5, p. 16504, 2015.

- [15] R. Santbergen, R. Mishima, T. Meguro, et al., “Minimizing optical losses in monolithic perovskite/c-Si tandem solar cells with a flat top cell,” *Optic Express*, vol. 24, no. 18, p. A1288, 2016.
- [16] J. Lehr, M. Langenhorst, R. Schmager, et al., “Energy yield modelling of perovskite/silicon two-terminal tandem PV modules with flat and textured interfaces,” *Sustainable Energy Fuels*, vol. 2, no. 12, pp. 2754–2761, 2018.
- [17] W. Qarony, M. I. Hossain, V. Jovanov, A. Salleo, D. Knipp, and Y. H. Tsang, “Influence of perovskite interface morphology on the photon management in perovskite/silicon tandem solar cells,” *ACS Appl. Mater. Interfaces*, vol. 12, no. 13, pp. 15080–15086, 2020.
- [18] F. E. Subhan, A. D. Khan, A. D. Khan, N. Ullah, M. Imran, and M. Noman, “Optical optimization of double-side-textured monolithic perovskite–silicon tandem solar cells for improved light management,” *RSC Adv.*, vol. 10, no. 45, pp. 26631–26638, 2020.
- [19] D. Chen, P. Manley, P. Tockorn, et al., “Nanophotonic light management for perovskite–silicon tandem solar cells,” *J. Photon. Energy*, vol. 8, p. 022601, 2018.
- [20] K. A. Bush, S. Manzoor, K. Frohna, et al., “Minimizing current and voltage losses to reach 25% efficient monolithic two-terminal perovskite–silicon tandem solar cells,” *ACS Energy Lett.*, vol. 3, no. 9, pp. 2173–2180, 2018.
- [21] M. Jošt, E. Köhnen, A. B. Morales-Vilches, et al., “Textured interfaces in monolithic perovskite/silicon tandem solar cells: advanced light management for improved efficiency and energy yield,” *Energy Environ. Sci.*, vol. 11, no. 12, pp. 3511–3523, 2018.
- [22] L. Mazarella, Y. H. Lin, S. Kirner, et al., “Infrared light management using a nanocrystalline silicon oxide interlayer in monolithic perovskite/silicon heterojunction tandem solar cells with efficiency above 25%,” *Adv. Energy Mater.*, vol. 9, no. 14, p. 1803241, 2019.
- [23] E. Köhnen, M. Jošt, A. B. Morales-Vilches, et al., “Highly efficient monolithic perovskite silicon tandem solar cells: analysing the influence of current mismatch on device performance,” *Sustain. Energy Fuels*, vol. 3, pp. 1995–2005, 2019.
- [24] J. Xu, C. C. Boyd, Z. J. Yu, et al., “Triple-halide wide–band gap perovskites with suppressed phase segregation for efficient tandems,” *Science*, vol. 367, no. 6482, pp. 1097–1104, 2020.
- [25] F. Sahli, J. Werner, B. A. Kamino, et al., “Fully textured monolithic perovskite/silicon tandem solar cells with 25.2% power conversion efficiency,” *Nat. Mater.*, vol. 17, no. 9, pp. 820–826, 2018.
- [26] G. Nogay, F. Sahli, J. Werner, et al., “25.1%-efficient monolithic perovskite/silicon tandem solar cell based on a p-type monocrystalline textured silicon wafer and high-temperature passivating contacts,” *ACS Energy Lett.*, vol. 4, no. 4, pp. 844–845, 2019.
- [27] Y. Hou, E. Aydin, M. De Bastiani, et al., “Efficient tandem solar cells with solution-processed perovskite on textured crystalline silicon,” *Science*, vol. 367, no. 6482, pp. 1135–1140, 2020.
- [28] B. Chen, Z. J. Yu, S. Manzoor, et al., “Blade-coated perovskites on textured silicon for 26%-efficient monolithic perovskite/silicon tandem solar cells,” *Joule*, vol. 4, no. 4, pp. 850–864, 2020.
- [29] E. Aydin, T. G. Allen, M. De Bastiani, et al., “Interplay between temperature and bandgap energies on the outdoor performance of perovskite/silicon tandem solar cells,” *Nat. Energy*, vol. 5, no. 11, pp. 851–859, 2020.
- [30] M. Jaysankar, M. Filipič, B. Zielinski, et al., “Perovskite-silicon tandem solar modules with optimised light harvesting,” *Energy Environ. Sci.*, vol. 11, no. 6, pp. 1489–1498, 2018.
- [31] A. S. Subbiah, F. H. Isikgor, C. T. Howells, et al., “High-performance perovskite single-junction and textured perovskite/silicon tandem solar cells via slot-die-coating,” *ACS Energy Lett.*, vol. 5, no. 9, pp. 3034–3040, 2020.
- [32] T. Kodalle, S. S. Schmidt, C. Wolf, et al., “Investigating sulfur distribution and corresponding bandgap grading in  $\text{Cu}(\text{In,Ga})(\text{S,Se})_2$  absorber layers processed by fast atmospheric chalcogenization of metal precursors,” *J. Alloys Compd.*, vol. 703, pp. 600–604, 2017.
- [33] U. W. Paetzold, W. Qiu, F. Finger, J. Poortmans, and D. Cheyns, “Nanophotonic front electrodes for perovskite solar cells,” *Appl. Phys. Lett.*, vol. 106, no. 17, p. 173101, 2015.
- [34] B. Shi, B. Liu, J. Luo, et al., “Enhanced light absorption of thin perovskite solar cells using textured substrates,” *Sol. Energy Mater. Sol. Cell.*, vol. 168, pp. 214–220, 2017.
- [35] K. Deng, Z. Liu, M. Wang, and L. Li, “Nanoimprinted grating-embedded perovskite solar cells with improved light management,” *Adv. Funct. Mater.*, vol. 29, no. 19, p. 1900830, 2019.
- [36] Y. Wu, C. Chen, H. Wang, et al., “Toward ultra-thin and full functional perovskite solar cells by broadband light scattering management and efficient interfacial modification,” *Sol. Energy Mater. Sol. Cell.*, vol. 206, p. 110297, 2020.
- [37] P. Tockhorn, J. Sutter, R. Colom, et al., “Improved quantum efficiency by advanced light management in nanotextured solution-processed perovskite solar cells,” *ACS Photonics*, vol. 7, no. 9, pp. 2589–2600, 2020.
- [38] C. Y. Xu, W. Hu, G. Wang, et al., “Coordinated optical matching of a texture interface made from demixing blended polymers for high-performance inverted perovskite solar cells,” *ACS Nano*, vol. 14, no. 1, pp. 196–203, 2020.
- [39] R. Schmager, I. M. Hossain, F. Schackmar, B. S. Richards, G. Gomard, and U. W. Paetzold, “Light coupling to quasi-guided modes in nanoimprinted perovskite solar cells,” *Sol. Energy Mater. Sol. Cell.*, vol. 201, p. 110080, 2019.
- [40] L. Gil-Escrig, M. Roß, J. Sutter, A. Al-Ashouri, C. Becker, and S. Albrecht, “Fully vacuum-processed perovskite solar cells on pyramidal microtextures,” *Sol. RRL*, vol. 5, p. 2000553, 2020.
- [41] J. Sutter, D. Eisenhauer, P. Wagner, et al., “Tailored nanostructures for light management in silicon heterojunction solar cells,” *Sol. RRL*, vol. 4, p. 2000484, 2020.
- [42] K. Jäger, C. Barth, M. Hammerschmidt, et al., “Simulations of sinusoidal nanotextures for coupling light into c-Si thin-film solar cells,” *Optic Express*, vol. 24, pp. A569–A580, 2016.
- [43] A. Razaq, V. Depauw, H. S. Radhakrishnan, et al., “Infrared absorption enhancement using periodic inverse nanopillars in crystalline-silicon bottom cells for application in tandem devices,” *IEEE J. Photovolt.*, vol. 10, no. 3, pp. 740–748, 2020.

- [44] H. H. Li, "Refractive index of alkali halides and its wavelength and temperature derivatives," *J. Phys. Chem. Ref. Data*, vol. 5, no. 2, pp. 329–528, 1976.
- [45] A. Tejada Esteves, Personal Communication. 2020.
- [46] L. Mazarella, M. Werth, K. Jäger, et al., "Infrared photocurrent management in monolithic perovskite/silicon heterojunction tandem solar cells by using a nanocrystalline silicon oxide interlayer," *Optic Express*, vol. 26, no. 10, p. A487, 2018.
- [47] K. Jäger, L. Korte, B. Rech, and S. Albrecht, "Numerical optical optimization of monolithic planar perovskite–silicon tandem solar cells with regular and inverted device architectures," *Optic Express*, vol. 25, no. 12, pp. A473–A482, 2017.
- [48] M. A. Green and M. J. Keevers, "Optical properties of intrinsic silicon at 300 k," *Prog. Photovoltaics Res. Appl.*, vol. 3, no. 3, pp. 189–192, 1995.
- [49] J. Pomplun, S. Burger, L. Zschiedrich, and F. Schmidt, "Adaptive finite element method for simulation of optical nano structures," *Phys. Status Solidi B*, vol. 244, pp. 3419–3434, 2007.
- [50] T. Tiedje, E. Yablonovitch, G. D. Cody, and B. G. Brooks, "Limiting efficiency of silicon solar cells," *IEEE Trans. Electron. Dev.*, vol. 31, no. 5, pp. 711–716, 1984.
- [51] P.-I. Schneider, X. Garcia Santiago, V. Soltwisch, M. Hammerschmidt, S. Burger, and C. Rockstuhl, "Benchmarking five global optimization approaches for nano-optical shape optimization and parameter reconstruction," *ACS Photonics*, vol. 6, no. 11, pp. 2726–2733, 2019.

---

**Supplementary Material:** The online version of this article offers supplementary material (<https://doi.org/10.1515/nanoph-2020-0674>).